© 2020. Published by The Company of Biologists Ltd | Journal of Experimental Biology (2020) 223, jeb224402. doi:10.1242/jeb.224402

RESEARCH ARTICLE

Whale sharks increase swimming effort while filter feeding, but appear to maintain high foraging efficiencies

David E. Cade[1,2,*], J. Jacob Levenson[3], Robert Cooper[4], Rafael de la Parra[5], D. Harry Webb[6] and Alistair D. M. Dove[6]

ABSTRACT

Whale sharks (*Rhincodon typus*) – the largest extant fish species – reside in tropical environments, making them an exception to the general rule that animal size increases with latitude. How this largest fish thrives in tropical environments that promote high metabolism but support less robust zooplankton communities has not been sufficiently explained. We used open-source inertial measurement units (IMU) to log 397 h of whale shark behavior in Yucatán, Mexico, at a site of both active feeding and intense wildlife tourism. Here we show that the strategies employed by whale sharks to compensate for the increased drag of an open mouth are similar to ram feeders five orders of magnitude smaller and one order of magnitude larger. Presumed feeding constituted 20% of the total time budget of four sharks, with individual feeding bouts lasting up to 11 consecutive hours. Compared with normal, sub-surface swimming, three sharks increased their stroke rate and amplitude while surface feeding, while one shark that fed at depth did not demonstrate a greatly increased energetic cost. Additionally, based on time-depth budgets, we estimate that aerial surveys of shark populations should consider including a correction factor of 3 to account for the proportion of daylight hours that sharks are not visible at the surface. With foraging bouts generally lasting several hours, interruptions to foraging during critical feeding periods may represent substantial energetic costs to these endangered species, and this study presents baseline data from which management decisions affecting tourist interactions with whale sharks may be made.

KEY WORDS: Bio-logging, Gigantism, Planktivores, Ram filter feeding, Swimming kinematics, *Rhincodon typus*

INTRODUCTION

As giant filter-feeding fishes, whale sharks (*Rhincodon typus* Smith 1828) fill an ecomorphological niche that is at least 165 million years old (Friedman et al., 2010), yet despite more than a century of study, there are major gaps in our understanding of their ecology (Rowat and Brooks, 2012), particularly when it comes to their feeding behavior and energetic budgets (Colman, 1997; Stevens, 2007). While early studies that observed these animals among schooling forage fish like sardines presumed that these animals were capturing fish to meet these high demands, the current consensus based on diet analyses and additional observations is that these animals primarily feed on small zooplankton such as copepods, coral spawn and fish eggs (reviewed in Motta et al., 2010; Rowat and Brooks, 2012), and that earlier observations of spatial associations (e.g. Duffy, 2002) were more likely observations of these giant predators foraging on the same prey as fish more than five orders of magnitude less massive (although see also Chen et al., 2002).

Three primary modalities of filter feeding have been noted in whale sharks around the world, all from surface-associated observations (Nelson and Eckert, 2007; Motta et al., 2010; Rowat and Brooks, 2012). The least energetically intensive appears to be vertical feeding (also known as 'bottling' or 'botelleando') whereby the shark stops swimming and appears to use active suction to bring small fish and zooplankton into its mouth. This feeding mode has been associated with lower overall zooplankton density than in active surface ram feeding (Nelson and Eckert, 2007), although we have observed vertical feeding when prey is patchily distributed in dense regions whose density may not be captured appropriately with net-sampling. Active surface feeding involves swimming slowly (<1 m s^{-1}) with open mouths and using pads anterior to the gills as filtration surfaces to retain prey while filtered water then passes through the gills (Motta et al., 2010). This foraging technique has convergently evolved in taxa as diverse (in form and size) as anchovies (Carey and Goldbogen, 2017), paddlefish (Sanderson et al., 1994; Haines and Sanderson, 2017), two additional shark species (Tomita et al., 2011; Carrier et al., 2012) and Balaenid whales (Simon et al., 2009; van der Hoop et al., 2019). Ram feeding in whale sharks has been additionally characterized as 'active' or 'passive' based on the apparent swimming effort spent while feeding at the surface or at depth, respectively (Nelson and Eckert, 2007; Motta et al., 2010), with surface feeding likely also involving active suction of prey (Gudger, 1941a). While the relative effort required for each of these foraging modes has not before been quantified, surface feeding should be more energetically costly due to increased wave drag when swimming at the surface (Blake, 2009). Similarly, we hypothesize that swim effort while ram filtration feeding, both at the surface and at depth, is more energetically costly than regular swimming due to resistance from water passing through the filter as well as increased drag from the open mouth (Vogel, 1994; Potvin and Werth, 2017). Indeed, increases in effort have been noted while foraging in two previous ram filtration kinematic feeding studies, in species as diverse as anchovies (Carey and Goldbogen, 2017) and baleen whales (van der Hoop et al., 2019).

Bio-logging inertial measurement units (IMU), developed for navigational systems and miniaturized for consumer applications, have been used more recently to quantify body orientation and motion in diverse taxa (e.g. Wright et al., 2014; Fossette et al.,

[1]Institute of Marine Science, University of California, Santa Cruz, 115 McAllister Way, Santa Cruz, CA 95060, USA. [2]Hopkins Marine Station, Stanford University, 120 Ocean View Blvd, Pacific Grove, CA 93950, USA. [3]US Department of Interior, Bureau of Ocean Energy Management, 1849 C Street, NW, Washington, DC 20240, USA. [4]Oceans Forward, 17 Hamilton St, Plymouth, MA 02360, USA. [5]Ch'ooj Ajauil AC, Av. Xelha 1 -311, Cancún, Q. Roo, México 77509. [6]Research and Conservation Department, Georgia Aquarium, 225 Baker St, Atlanta, GA 30313, USA.

*Author for correspondence (davecade@stanford.edu)

D.E.C., 0000-0003-3641-1242; R.C., 0000-0001-6213-7414; R.d.l.P., 0000-0003-1158-3523

Received 19 March 2020; Accepted 25 April 2020

2015; Noda et al., 2016; Gough et al., 2019), including initial studies on the swimming mechanics of whale sharks (Gleiss et al., 2011a, 2013; Meekan et al., 2015). Herein we build on these studies by using IMUs to differentiate foraging from non-foraging periods, examining the swimming mechanics in each behavioral mode, and presenting the first information on foraging rates of individual whale sharks over multi-day time scales. As the largest living ectotherm and, by extension, the largest ectothermic filter feeder, whale sharks represent the extreme end point for studies of the advantages and limitations of large body size across species, yet to our knowledge, this is the first study to examine sub-surface feeding behavior in whale sharks, and only recently have the kinematics of ram filtration been studied in any fish species (Carey and Goldbogen, 2017; Haines and Sanderson, 2017). In cetaceans, the ability to acquire resources in bulk via filter feeding has been shown to be a likely driving force in the evolution of large body sizes (Slater et al., 2017; Goldbogen et al., 2019), but the thermal needs of sharks combined with limited prey availability in the tropics is thought to limit the body size of sharks in contemporary oceans (Meekan et al., 2015); here we describe information on foraging rates and foraging costs that can help us to understand these ecological trade-offs.

When their zooplanktonic prey form extensive, dense patches near shore that increase the efficiency of feeding, whale sharks in tropical and subtropical regions around the world have been observed forming large feeding aggregations (Hoffmayer et al., 2007; de la Parra Venegas et al., 2011), often composed predominantly of sub-adult males (Rowat and Brooks, 2012; Ketchum et al., 2013; Norman et al., 2017). These slow-swimming, non-aggressive aggregations of the world's largest fish predictably attract sizable aggregations of human tourists whose visits are major components of local economies. In Australia, for instance, the value for each living whale shark was conservatively calculated at UA$282,000 per shark (Norman and Catlin, 2007). The nature of wildlife tourism opportunities varies widely between sites, based on both characteristics of the aggregations and anthropocentric factors such as the level of local economic development and the size of the available tourist market. Potential impacts can be obvious, e.g. in some locations whale sharks are given food by tour operators (Brena et al., 2015; Schleimer et al., 2015), or more subtle such as changes in shark behavior when tourists are nearby. Whale shark tourism in Yucatán, Mexico, the site of investigation in this study, has been ineffectively regulated and has grown rapidly from a few boats operating out of Isla Holbox in 2004, to 240 boats currently operating out of Holbox, Isla Mujeres and Cancún. The increasing interactions of human tourists with this endangered species have thus prompted questions about the impacts of intensive tourism on the behavior of these animals, particularly if tourists are interrupting feeding behavior during a critical period of energy acquisition. Additionally, estimates of abundance of these populations rely on aerial surveys, but no quantitative measurements of time budgets at various depths in this region have been put forward, potentially leading to biases in population size estimates. Understanding fine scale animal behavior relative to potential anthropogenic threats is vital for informed natural resource management and to design potential mitigation options; this study sought to shed light on whale shark foraging behaviors in a highly touristic region.

MATERIALS AND METHODS

Ethics statement

The study reported here was approved by the Conservation Research and Animal Care Committee at the Georgia Aquarium on 8 June 2009. Field work was conducted with permission of the Mexican Federal Government under permits from Dirección General de Vida Silvestre (the General Directorate of Wildlife), number SGPA/DGVS 10048/12.

Study area and population

The world's largest known seasonal aggregation of whale sharks occurs in waters between Cabo Catoche and Isla Mujeres, at the northeastern tip of the Yucatán Peninsula in Mexico, beginning in May and dispersing in mid-September (de la Parra Venegas et al., 2011). This site has become one of the most intense foci for whale shark tourism as well as commercial photography due to the proximity of the event to the major tourist city of Cancún, combined with the extraordinary size of the event and the warm clear blue water in which it occurs. This event, colloquially known as 'the Afuera aggregation' (Spanish: 'outside' or 'offshore' aggregation) involves predominantly juvenile and sub-adult whale sharks in a sex ratio of roughly three males to one female (de la Parra Venegas et al., 2011). The Afuera aggregation is a feeding event that, similar to other aggregations of whale sharks (e.g. Hoffmayer et al., 2007), has historically focused on concomitant mass spawning of little tunny, *Euthynnus alleteratus*, known locally as bonito. The mass spawning event has not been directly observed at this location, but the aggregation has been noted to occur in water replete with eggs genetically matched to little tunny (de la Parra Venegas et al., 2011).

Tag deployment and programming

The OpenTag (Loggerhead Instruments, Palmer Park Cir, Sarasota, FL, USA; Ware et al., 2016) is an Arduino-compatible open-source IMU for recording high-frequency motion sensor data to a microSD memory card. Three-axis gyroscopes, accelerometers and magnetometers were sampled at 50 or 100 Hz, while depth and temperature were sampled continuously at 1 Hz. The rechargeable lithium battery allowed for deployments of at least 7 days, sampling the IMU at 100 Hz.

Previous researchers have recommended a direct body attachment near the caudal peduncle for the best measurement of tail beat frequency (Whitney et al., 2007), while other whale shark studies have attached accelerometer tags directly to the second dorsal fin (Gleiss et al., 2009). We selected the first dorsal fin as an attachment site as a compromise between calculating average body position (for which anteriorly placed tags give less overall motion) and tail beat frequency measurement, at the same time providing a consistent attachment point for comparisons between animals. The tag was recessed in a shaped syntactic foam float to create positive buoyancy for tag recovery, and attached using an elastic band system (Fig. 1). In 2013, the tag–float unit was attached to a bicycle inner tube using plastic cable ties. In 2014 and 2015, the tag–float unit was attached to an elastic bungee cord with a cinch closure, also by using plastic cable ties. A section of plastic teeth from a dog's pinch-training collar was included in the loop in 2014 and 2015 to provide friction attachment on the leading edge of the dorsal fin (Fig. 1). A burn wire or galvanic timed release were incorporated into the tag to allow for a release time to induce detachment, and a VHF tag (animal telemetry system) aided in locating the tag at the surface for recovery.

Tags were applied to the animal by two-person teams of snorkelers. One snorkeler swam along either side of the whale shark, and the first snorkeler placed part of the elastic loop under the free end of the first dorsal fin, while the other snorkeler stretched the elastic over the apex of the dorsal fin and situated the plastic teeth on

Journal of Experimental Biology (2020) 223, jeb224402. doi:10.1242/jeb.224402

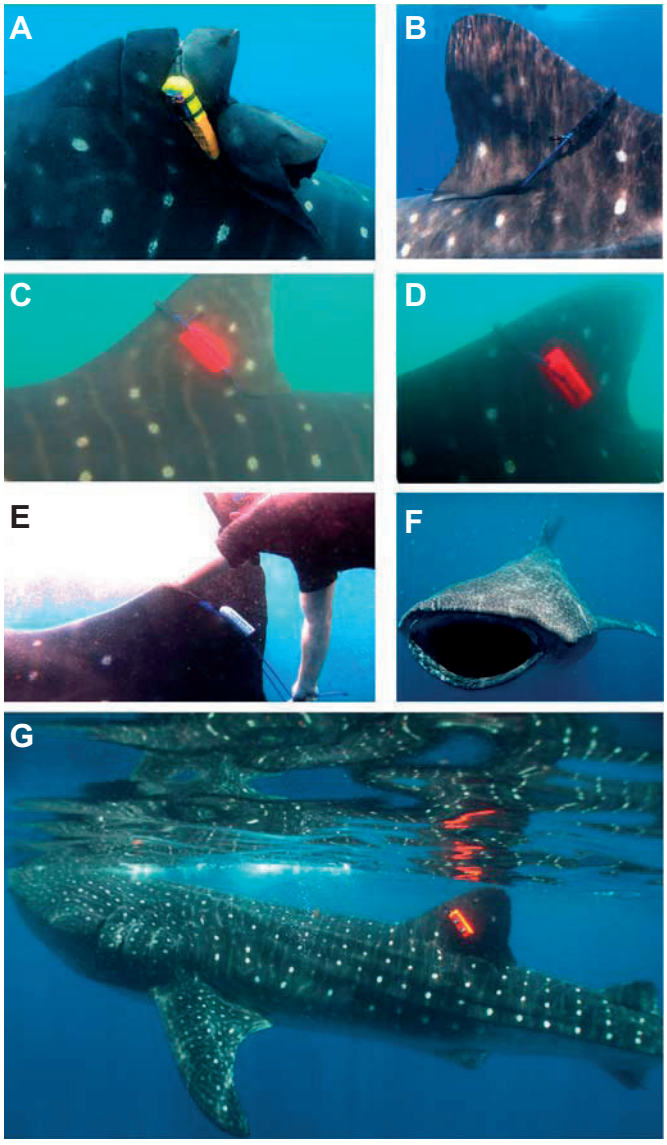

Fig. 1. Attachment of OpenTags to whale sharks near the Afuera whale shark aggregation off Cancún, Mexico. (A–D) Tags affixed to the four sharks used in this study (MXA-047, MXA-522, MXA-1275 and MXA-406, respectively). (E) The process of affixing a tag using the elastic band. (F) Ram filtration feeding in whale sharks involves swimming forward slowly with the mouth open. (G) A tagged shark in profile, showing the size of the tag in relation to the size of the shark.

the leading edge of the fin, such that the tag–float unit was pressed flat against the side of the dorsal fin. Minor adjustments to the positioning of the tag on the animal were occasionally made post-deployment (an advantage to working with a slowly swimming animal that allows human approaches).

One tag was deployed in 2013, five in 2014 and six in 2015 (Fig. 2). Of the recovered tags, four had data that could be read, all of which were from whale sharks identified in the international whale shark Wildbook found at www.whaleshark.org. The 2013 tag (deployed on shark identified as MXA-047) recorded accelerometry (acc) data at 50 Hz and pressure at 1 Hz, the 2014 tag (MXA-522) recorded acc data at 100 Hz and pressure at 1 Hz, and the two 2015 tags (MXA-1275 and MXA-406) recorded acc data at 50 Hz and pressure at 10 Hz. Sharks will be referred to throughout by the number following 'MXA'.

Data extraction and analysis

Raw files were extracted from the tags and converted to csv files using open source dsg2csv software provided from Loggerhead instruments. The csv files (one file for the inertial sensors and a separate file for the pressure and temperature sensors) were read into MATLAB and pressure was up-sampled to match the sample rate of the accelerometer for each deployment. Files were time-synchronized, and gaps in time between each csv file (approximately 1–2 s every hour) created during file write were filled with linear interpolations between points. The custom MATLAB script for importing OpenTag data and aligning the different data streams regardless of sample rate is available from https://purl.stanford.edu/dp151fd3984. All sensors were initially calibrated using manufacturer specifications and then an *in situ* calibration procedure was applied to the accelerometer and magnetometer data using tools from animaltags.org.

Data were down-sampled to 10 Hz, and tag frame was rotated to shark frame by examining periods at the surface where the shark was assumed to be in a level position. Occasionally the tag rotated in its attachment, and different calibrations were applied to each section of tag stability. Animal pitch, roll and heading were calculated via custom MATLAB scripts (Johnson and Tyack, 2003; Cade et al., 2016). Speed is a critical metric of swimming effort, but our device did not have a dedicated speed sensor. Relative speed was calculated from the accelerometer (Cade et al., 2018), but could not be linked to actual speed as shark speeds did not typically exceed the floor of the detection method (~1 m s^{-1}) to sufficiently calibrate the curves, so speed was excluded from further analyses. Pseudotracks, an animal's position in space resulting from integrated dead-reckoning of animal orientation and motion, were created using animal pitch, heading and an estimated speed of 1 m s^{-1} and plotted in three dimensions (3D) using Trackplot (Ware et al., 2006).

Identification of foraging

Although information on the kinematics and behavioral strategies of ram filtration feeding are sparse, van der Hoop et al. (2019), studying ram feeding right whales (*Eubalaena glacialis*), noted high variability in the heading of feeding animals, presumably as animals adjusted their path to maintain position in dense portions of the school. Whale sharks feeding at the surface have been observed using similar techniques (Nelson and Eckert, 2007; Motta et al., 2010), and similar behavior was easily identified in the Trackplots created from the 3D pseudotracks, as well as in plots of animal orientation (Fig. 3). Although we could not directly observe mouth gape with our tags, unless our sharks were exhibiting a heretofore unnoted behavioral mode, the most parsimonious explanation for these periods of increased track tortuosity is that they coincided with foraging effort, so we identified periods with highly tortuous tracks coincident with increased stroking effort as 'feeding' (Figs 3 and 4), and analysed these presumed feeding and non-feeding periods independently.

Tortuosity (τ) of shark tracks was calculated in 10 min bins (from positions p_1 to p_2 at times t_1 to t_2), following the definition from Wilson et al. (2007) such that a straight line track would have τ=0 and a circular track would have τ=1:

$$\tau = 1 - \frac{\text{distance from } p_1 \text{ to } p_2}{\text{distance traveled from } t_1 \text{ to } t_2}. \quad (1)$$

This is equivalent to 1 – (distance made good/stretched-out track length).

To identify individual tail beat amplitude (in radians), body heading (mean yaw in the global reference frame) was calculated from the low-pass filtered (0.05 Hz) shark-frame oriented magnetometer signal, then subtracted from the heading calculated

Journal of Experimental Biology (2020) 223, jeb224402. doi:10.1242/jeb.224402

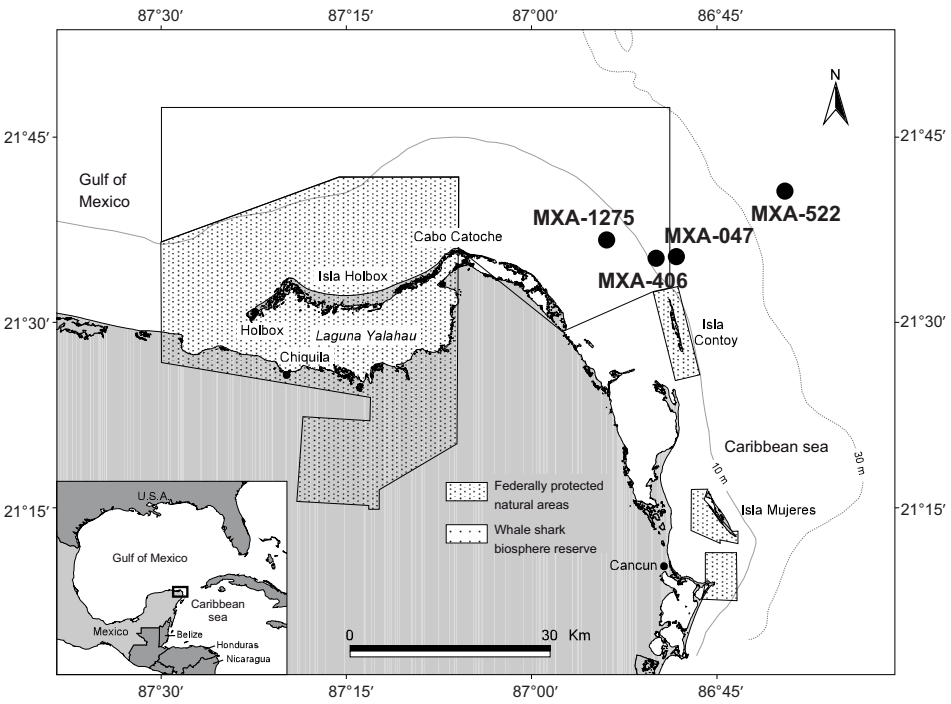

Fig. 2. Map of study area. Locations of tag deployments used in this study are indicated alongside the shark identity (Table 1). Map copyright: John Tyminski and Rafael de la Parra.

from the magnetometer low-pass filtered at 0.5 Hz. Tail beat rotation speed was calculated from the z-axis gyroscope signal (low-pass filtered at 0.5 Hz). Individual tail beats and gliding periods were identified by inputting the tail beat amplitude signal to the stroke_glide tool at animaltags.org, using a threshold of five degrees and a maximum duration of 15 s. Tail beat kinematics (rotation rate, amplitude) were normally distributed, so values that were more than three standard deviations (s.d.) away from the mean were excluded from analysis as likely noise artefacts. Overall dynamic body acceleration (ODBA) was calculated at each time step following Gleiss et al. (2011b).

Sharks and other ectothermic fish are known to conduct V-shaped (so-called because of their appearance on time–depth profiles) bounce dives where they move up or down in the water column and then return to their previous depth (Gleiss et al., 2011a). These features were apparent in our data, and we defined bounce dives in whale sharks as excursions of 10 m or more from the overall depth profile smoothed with a 10 min running mean filter.

Metabolic cost of foraging

Mass-specific metabolic rate ($\dot{M}_{O_2}$, measured as mg O_2 consumed per kilogram of body mass per hour) has been shown to increase linearly with ODBA in sharks, with a slope of increase that decreases with body size, but which is independent of ambient temperature (Lear et al., 2017). To estimate the relationship between increased ODBA and increased $\dot{M}_{O_2}$ for whale sharks, we performed a power regression using the midpoint of the range of masses of the three shark species measured at high temperature in Lear et al. (2017) to yield a mass dependent relationship of:

$$\frac{\Delta\dot{M}_{O_2}}{\Delta\text{ODBA}} = 954.3 \times M^{-0.4342}, \quad r^2 = 0.879, \qquad (2)$$

where M is shark mass and ODBA is measured in $\boldsymbol{g}$, the acceleration due to gravity. Because ODBA is subject to a variety of externalities (Wilson et al., 2020), which in our case are driven by noise derived from tag placement on non-rigid dorsal fins, ODBA was only compared within a feeding regime (i.e. surface ODBA was not compared with sub-surface ODBA). Shark mass was expressed as a function of shark length using the length (L)–mass (M) relationship from Hsu et al. (2012):

$$M = 12.1 \times L^{2.862}. \qquad (3)$$

Then, the equivalent amount of zooplankton (g h^{-1}) that would need to be consumed is a linear multiplier of $\dot{M}_{O_2}$:

$$\text{Zooplankton} = \frac{\dot{M}_{O_2}}{1290} \times 20.55 \times 0.9^{-1} \times 1.357^{-1} \times M, \qquad (4)$$

where 1290 is the conversion from mg O_2 to liters of O_2 at 29°C, 20.55 converts liters of O_2 burned to kJ (McArdle et al., 2010), 0.9 is a representative assimilation efficiency for sharks (Kao, 2000; Leigh et al., 2017), and 1.357 is a mean caloric value of zooplankton (in kJ g^{-1}) found near foraging whale sharks (Motta et al., 2010). To calculate how much volume a shark of a given size would filter per hour, a regression of mouth area and total length from Motta et al. (2010) yields:

$$\text{Mouth area} = 0.006803 \times L^{1.856}, \quad r^2 = 0.999. \qquad (5)$$

Although shark mouths may be dynamic while foraging, we assumed that typical foraging involved this average gape area. Assuming a forward motion speed of 1 m s^{-1} allowed for the volume of water filtered per unit time to be estimated.

RESULTS

General behavior

Ten whale sharks were fitted with OpenTags from 2013 to 2015. Of these, six recorded some data and four had data that could be appropriately decoded into engineering units (Table 1). Deployment lengths of these tags ranged from 45 to 189 h and all tags were deployed by a diver in shallow water (<3 m depth). Periods consistent with foraging behavior comprised 16, 16, 6 and 26% of the deployment durations for the four sharks (Table 1). Foraging bout durations, defined as total periods with <10 min

Journal of Experimental Biology (2020) 223, jeb224402. doi:10.1242/jeb.224402

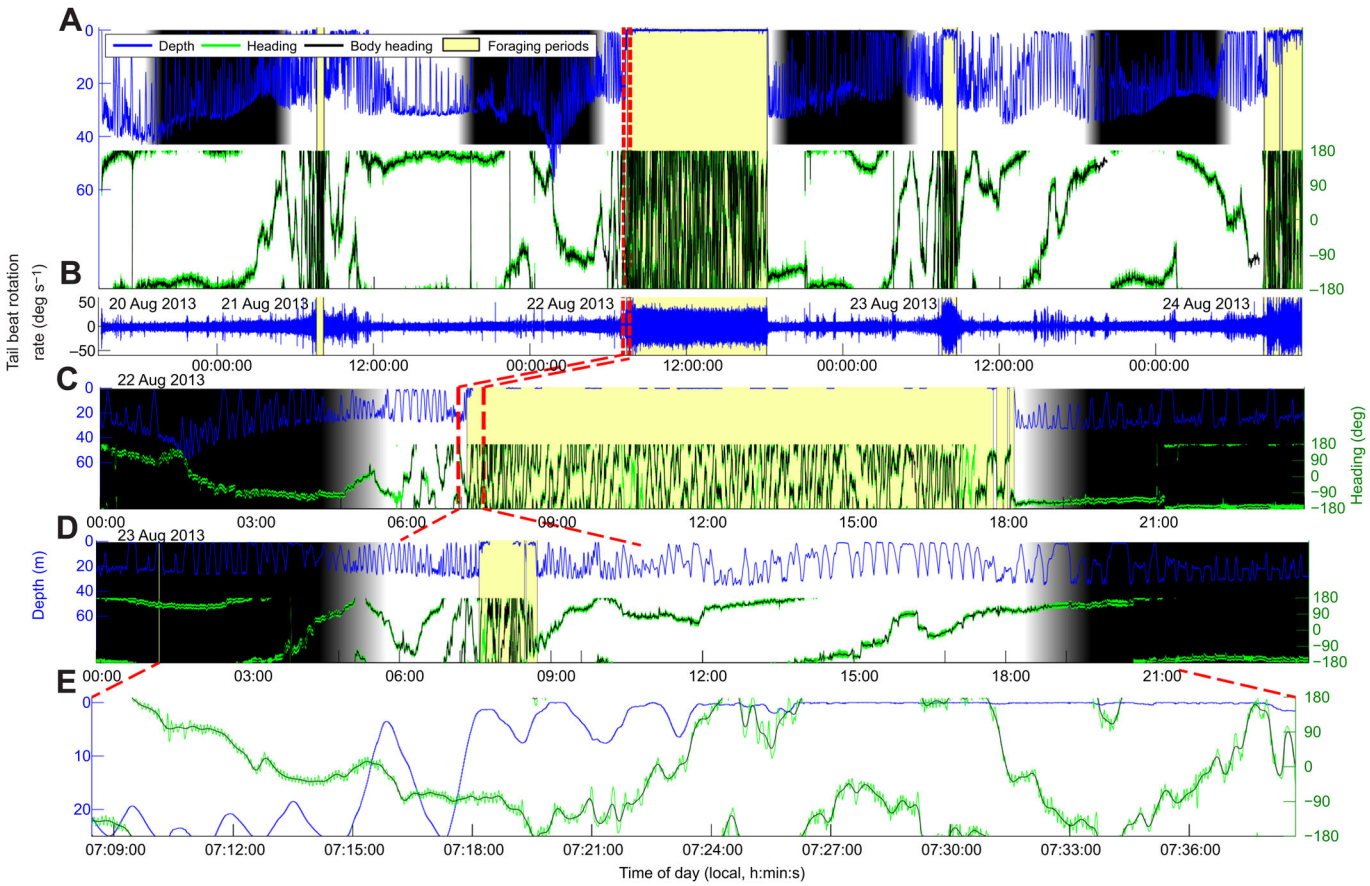

Fig. 3. Plot of tail beat kinematics of MXA-047. Dark areas in all figures represent night-time. (A) Depth profile and heading across the entire deployment. Presumed feeding periods are highly tortuous with abundant heading changes. (B) Tail beat rotation rate. Strokes are faster during presumed feeding periods. (C) Detailed plot of depth and heading from 22 August 2013. (D) Detailed plot from 23 August 2013. (E) Further zoomed-in plot of a transition to feeding on 22 August 2013; individual tail beats and their amplitude (variations from the smoothed body heading).

breaks in presumed foraging, ranged from less than a minute to 10.9 h, with per shark means (±s.d.) that ranged from 0.3±0.4 h in shark 1275 to 2.3±3.0 h for shark 522. Sharks varied in their foraging behavior. Despite long deployment durations, all of which were at least 45 h long, one shark (1275) demonstrated behavior consistent with feeding for only 6% of the tag duration, three sharks (047, 522 and 1275) demonstrated feeding behavior at the surface (<3 m tag depth) for >99% of their foraging effort (mean foraging depth 0.7±2.2, 0.1±0.4 and 1.1±1.5 m, respectively), and one shark (406) foraged primarily at depth (mean 24.0±4.2 m). Overall, the four sharks spent 32±20% of their time during daylight hours within 3 m of the surface, and 27±31% of the time within 3 m of the surface at night, with three of the four sharks spending more time at the surface during the day (Table 1, Fig. 5).

Sharks also showed diversity in the degree to which they exhibited diel variation (Table 1). While shark 047 spent 32% of the observed daylight hours foraging, it did not forage at night. In contrast, shark 522 spent 20% of its time foraging during the day and 12% at night, while 406 spent a greater proportion of its night-time hours foraging (21% during the day, 32% at night).

All sharks were tagged in a shallow water environment with water depths ranging from 20 to 40 m. Despite demonstrating foraging behavior at different depths, mean depths for the duration of the deployment were similar for three of the four sharks, and even shark 1275 that spent more than half of its time at the surface (Table 1) still spent 17% of its time below 10 m. Maximum depths for the four sharks were 57, 41, 28 and 28 m. All sharks would regularly perform 'bounce dives', both starting at depth and ascending and starting near the surface and descending (N=370 total ascent bounces and 424 descent bounces), and these bounce dives were of similar magnitude among all sharks (13.0±2.2 m for ascents, 13.2±2.5 m for descents).

Kinematics of foraging

In this region for these deployments, vertical feeding was identified as periods with body pitch >15 deg at a depth of <5 m with a reduction in swimming identified by periods with at least 1.5 times the mean non-feeding tail beat period between tail beats. This 'bottling' behavior was noted for a total of 219 s in shark 047 and 19 s in shark 522 (<1% of total foraging time in both cases). Sharks 047, 522 and 1275 had behavior consistent with feeding only at or close to the surface, while shark 406 fed primarily at depth (Table 2, Fig. 6). Mean tail beat period was on average 10% smaller during feeding than for non-feeding periods (Figs 5 and 6; Table 2), while the amplitude of rotation at the point of measurement (the dorsal fin) was on average 65% higher for the three surface-feeding sharks, but only 12% higher for the deep-feeding shark (Fig. 5). Similarly, the speed of tail rotation (in deg s^{-1}), was on average 66% faster during feeding for the surface-feeding sharks, but only 21% faster for the deep-feeding shark.

For all deployments, mean ODBA (hereafter referred to just as ODBA) during non-feeding stroking (0.41 m s^{-2}) was 2.3 times ODBA during gliding (0.18 m s^{-2}), which should be representative

Journal of Experimental Biology (2020) 223, jeb224402. doi:10.1242/jeb.224402

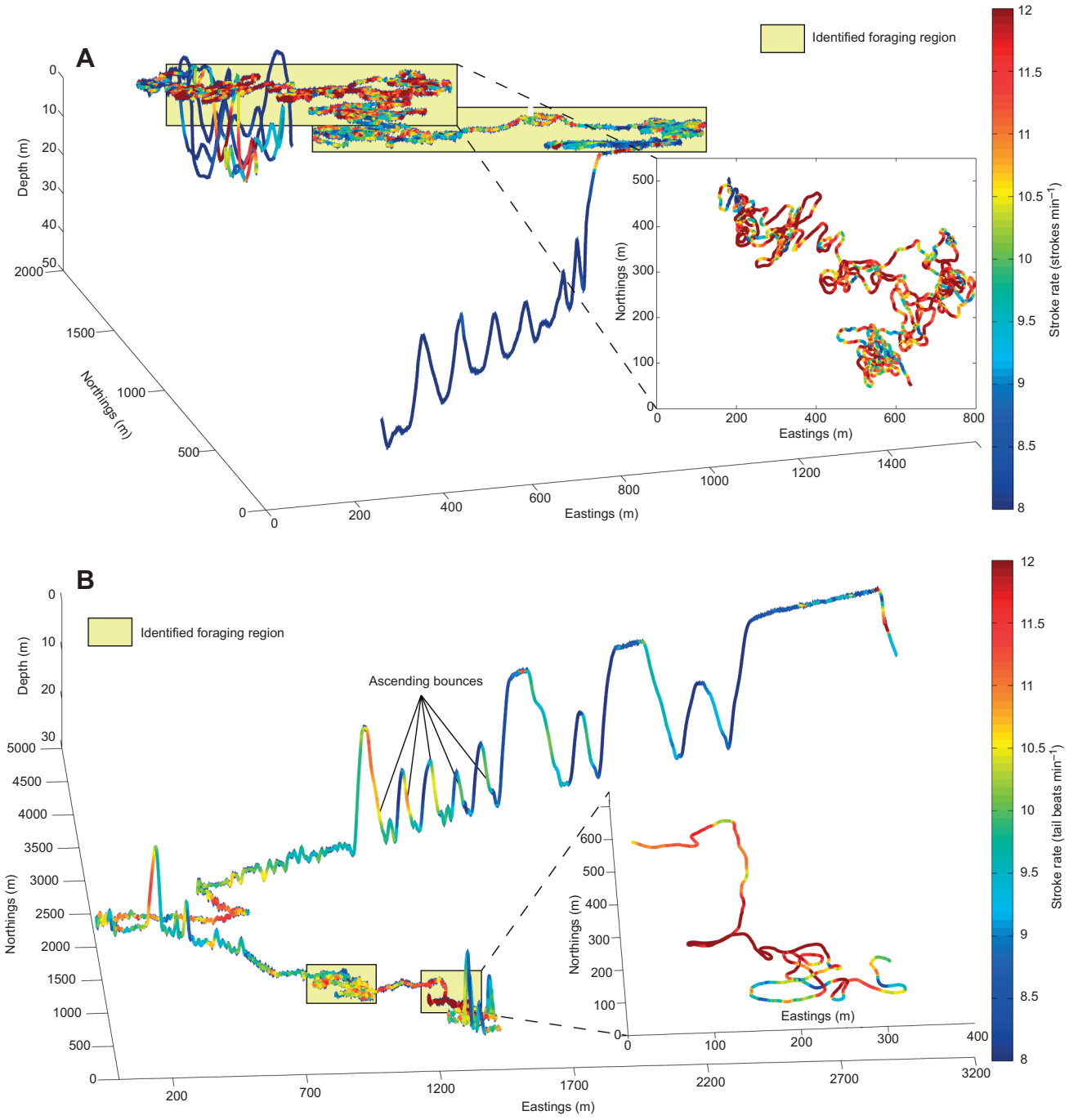

Fig. 4. Whale shark pseudotracks, assuming 1 m s^{-1} swimming speed. Partial tracks of MXA-047 (A) and MXA-406 (B) showing apparent surface feeding and feeding at depth, respectively. Tortuosity of the tracks is evident, as is the increased oscillatory rate during foraging. Both sharks showed an increase in oscillatory rate on ascents, consistent with behavior of negatively buoyant sharks (Gleiss et al., 2011a).

of the overall noise in the tag. For all sharks, surface feeding had ODBA (1.78 m s^{-2}) two times higher than non-feeding periods (0.87 m s^{-2}) at the surface (Fig. 6). Mean tortuosity of feeding periods was seven to 28 times higher in feeding periods compared with non-feeding periods (Fig. 5).

Feeding orientation

Sharks 047 and 522 were primarily oriented east–west when foraging, while shark 1275 was more uniform in distribution and shark 406, with a mean foraging depth of 24 m (Table 1B), was primarily oriented north-east (Fig. 7). Non-feeding periods for shark 047 were strongly biased south, shark 522 was strongly biased south-east, shark 406 was primarily between south-west and south-east, and shark 1275 had five distinct directions.

Foraging cost

For both presumed deep feeding and presumed surface feeding, the increased ODBA associated with foraging implied a commensurate increase in metabolic rate compared with non-feeding periods (Fig. 8A). The increased cost of foraging at the surface (from a mean ODBA increase of 0.92 m s^{-2}) was 3.4 times larger than the increased cost of foraging at depth (mean ODBA increase of

Journal of Experimental Biology (2020) 223, jeb224402. doi:10.1242/jeb.224402

Table 1. Tag deployment information

Shark no.	Shark ID	Sex	Date	Deployment duration (h)	Foraging duration (h)	Percentage of day spent foraging	Percentage of night spent foraging	Mean daytime depth (m)	Mean night-time depth (m)	Percentage of time spent <3 m (day)	Percentage of time spent <3 m (night)
1	MXA-047	F	20 August 2013	92.1	15.1	32%	0%	14.0±13.1	20.6±10.6	39%	12%
2	MXA-522	M	26 June 2014	71.0	11.7	20%	12%	17.4±11.1	18.0±10.8	23%	16%
3	MXA-1275	M	28 June 2015	45.4	2.5	10%	1%	6.1±7.7	2.7±3.4	56%	72%
4	MXA-406	M	2 July 2015	189.0	48.4	21%	32%	19.3±8.4	21.0±7.1	9%	7%

Values are listed as means±s.d.; F, female; M, male.

0.27 m s^{-2}). The amount of zooplankton that would have to be consumed to account for this increased foraging cost is similarly lower for deep feeding than for surface feeding (Fig. 8B).

DISCUSSION

Whale sharks are the largest extant fish and have a filtering apparatus unique to its species (Gudger, 1941a; Taylor et al., 1983; Motta et al., 2010). Due to their large size, and consequent metabolic requirements in tropical seas, it was presumed for many years that their diet must consist of larger prey (Gudger, 1941b; Duffy, 2002; Motta et al., 2010). More recent observations of morphology (Taylor et al., 1983) and observations of behavior (Motta et al., 2010) have since confirmed that these animals are strictly filter feeders (Gill, 1905). The degree to which small fish may be irregular parts of whale shark diets is at this point still undetermined (Rowat and Brooks, 2012); however, the low speeds observed in this study provide additional evidence that these large animals are primarily filter feeding on zooplankton, as filter feeding on highly maneuverable forage fish is typically observed to be successful only as part of the high-speed engulfment filtration feeding of rorqual whales (Sanderson and Wassersug, 1990) that essentially use surprise attacks to delay the dispersion of maneuverable prey (Cade et al., 2020). Filter feeding on aggregations of small but plentiful organisms is an efficient way to transfer energy across trophic levels. Due to this efficiency, filter feeding is ubiquitous at the largest body sizes in the oceans (Gearty et al., 2018; Goldbogen, 2018; Goldbogen et al., 2019; Lawson et al., 2019; Williams, 2019). Despite decades of interest and a rapidly increasing draw as a tourist attraction over the last two decades (Norman and Catlin, 2007), there is no published information on the energetic costs of this foraging style in whale sharks, and it is that hole that we sought to fill with this study.

Most studies of metabolic expenditure in swimming animals have found, or presumed, that all else being equal it takes about the same amount of energy to move a given fish mass forward a given distance at a given speed (e.g. Schmidt-Nielsen and Knut, 1984; Carlson et al., 2004; Gleiss et al., 2011a). Two characteristics of feeding in whale sharks, however, incur additional energetic costs above normal swimming modes. Continuous ram filtration feeding, even if performed passively, always incurs additional energetic costs compared with normal swimming due to the increased drag of water flow through a filter, and this is compensated for with increased stroke amplitudes, stroke rates, decreased speeds or decreased distance traveled per stroke while filtering (Sanderson and Wassersug, 1990; Sims, 2000; Carey and Goldbogen, 2017; van der Hoop et al., 2019). The most commonly observed whale shark filter feeding mode in the literature is active ram feeding at the surface (Nelson and Eckert, 2007; Motta et al., 2010). Although these reports may be biased by the limitations of surface-based observations, in this study we noted that three of four feeding sharks used this mode exclusively for more than 90% of the 30 logged hours of putative feeding. Swimming close to the surface is known to increase drag and, thus, swimming costs (Blake, 2009), and we observed higher costs of foraging for the three sharks feeding at the surface compared with the shark feeding at depth, as measured by tail beat amplitude, tail beat rotation rate and ODBA (Fig. 6).

The few ram filtration feeding species that have been studied all appear to compensate for the increased drag of filtering in similar ways. Northern anchovies (*Engraulis mordax*), despite the dangers of falling behind their school, slow down by 18% when filter feeding and switch gaits from the normal beat-glide gait to a continuously stroking motion while foraging. Each stroke during normal swimming is completed in 0.72 s, while each stroke while ram feeding takes 0.29 s, and anchovies move three times as far

Table 2. Surface and sub-surface foraging energetics

				At depth (>3 m)				At surface (<3 m)			
	Shark no.	Shark ID	Mean foraging depth (m)	Tail beat period (s)	Tail beat amplitude (deg)	Tail beat rotation rate (deg s^{-1})	ODBA (m s^{-2})	Tail beat period (s)	Tail beat amplitude (deg)	Tail beat rotation rate (deg s^{-1})	ODBA (m s^{-2})
Non-feeding	1	MXA-047	0.7±2.2	6.9±1.5	20.4±3.1	6.0±1.6	0.3±0.3	6.8±1.8	23.9±5.5	7.2±1.7	1.0±0.7
	2	MXA-522	0.1±0.4	7.7±1.6	14.3±2.0	2.8±1.3	0.2±0.1	7.8±2.3	16.3±3.9	4.0±1.5	0.7±0.6
	3	MXA-1275	1.1±1.5	7.2±1.0	18.7±4.3	4.8±2.6	0.2±0.2	7.6±1.6	20.5±5.9	9.4±2.7	0.9±0.7
	4	MXA-406	24.0±4.2	5.8±1.2	19.6±3.6	5.2±1.6	0.3±0.2	6.6±1.5	23.3±5.9	7.2±2.0	1.0±0.7
Feeding	1	MXA-047	0.7±2.2	*7.9±3.1*	*31.6±9.3*	*8.8±2.3*	*0.9±0.8*	6.0±2.3	32.4±17.7	10.0±2.1	1.9±1.4
	2	MXA-522	0.1±0.4	n/a	n/a	n/a	n/a	6.0±2.1	29.3±7.2	6.0±1.7	2.1±1.9
	3	MXA-1275	1.1±1.5	*8.4±1.7*	*29.6±6.1*	*6.4±2.5*	*0.4±0.5*	7.5±2.4	28.2±6.1	10.5±3.3	1.4±1.1
	4	MXA-406	24.0±4.2	5.5±1.1	22.3±4.2	6.3±1.7	0.3±0.2	5.3±1.8	26.8±6.5	7.8±2.4	1.7±1.3

Values are listed as means±s.d.; n/a, not applicable. Italicized values were calculated for sharks that spent <1% of their time foraging at depth.

Journal of Experimental Biology (2020) 223, jeb224402. doi:10.1242/jeb.224402

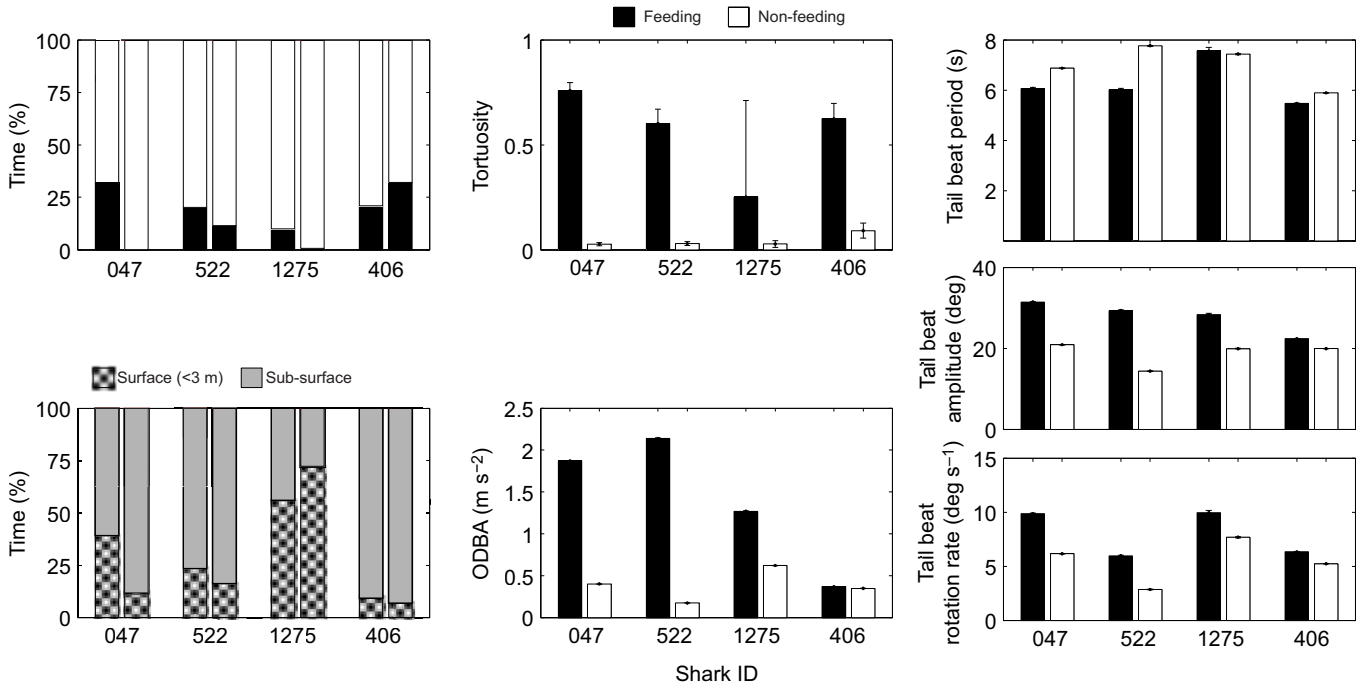

Fig. 5. Summary information of presumed feeding and non-feeding periods. Error bars are 95% confidence intervals.

for each stroke when normal swimming, while mean tail beat amplitudes (as determined by head yaw) was not significantly different (Carey and Goldbogen, 2017). Atlantic Menhaden, in contrast, swam 2.4 to 3.5 times faster when filter feeding, but compensated for the increased speed with higher than expected oxygen utilization (Durbin et al., 1980). At the larger end, North Atlantic right whales in the Bay of Fundy were shown to slow down while foraging by 21% from their descent speeds, yet stroke twice as fast and use strokes with more rotation to obtain the lower speed. Ascent speeds were similar to descent speeds, but stroke rates and amplitude were comparable to those employed when foraging (van der Hoop et al., 2019), probably due to fighting against buoyancy forces. Filtering drag increases with both the area of the filter and with the square of speed (Vogel, 1994), implying that these right whales were fighting against filtering drag to obtain slower speeds with more effort. Indeed, larger whales were observed to swim more slowly while filtering (van der Hoop et al., 2019). Whale sharks also forage at slow speeds $\leq$1 m s^{-1} (this study; Hoffmayer et al., 2007; Nelson and Eckert, 2007; Motta et al., 2010), and we found that whale sharks, similar to right whales, increase their stroke amplitude during ram filtration, and like both previously studied species, decrease the period of each stroke (Fig. 5).

Despite these increased costs of swimming while foraging, we found that the actual prey densities required to make up for the costs of foraging are relatively low, supplying evidence that the mass-specific metabolic costs of filter feeding may be low at large body sizes (Yowell and Vinyard, 1993). Assuming that sharks in regions where prey densities have been measured (e.g. Motta et al., 2010; where mean near-surface zooplankton density was 4.5 g m^{-3}) have similar energetic expenditures, whale sharks appear to have foraging efficiencies, defined as the energy from captured prey divided by expended energy, around 30 to 40. However, this value is only accounting for the cost of foraging over non-foraging at the same depth. Swimming at the surface is known to incur extra costs due to drag at the air–water interface (Blake, 2009). The measured difference in ODBA between surface foraging and surface non-foraging was approximately equivalent to the ODBA difference between surface non-foraging and sub-surface non-foraging periods (Table 2), implying that foraging efficiency would be cut in half; however, this interpretation should be treated with caution as at the surface the sharks' dorsal fins were often above the water surface and un-supported, potentially creating increased tag motion that increases at a different rate than for motion at depth. Regardless, foraging efficiencies appear to be approximately equivalent to other large ram feeders (e.g. bowhead and right whales; Goldbogen et al., 2019), and the low increase in energetic cost of foraging at depth compared with regular swimming at depth appears to allow foraging even at extremely low prey concentrations; indeed, Nelson and Eckert (2007) report prey concentrations approximately one-tenth as dense when sub-surface feeding by whale sharks was observed compared with when active surface feeding was observed.

The one shark that exhibited substantial sub-surface feeding also exhibited highly biased north-east orientation when foraging (Fig. 7). The prevailing sub-surface currents in this region are northerly (Kjerfve, 1994; Merino, 1998), so it is likely that this shark was orienting itself against the current to help aid prey capture under low prey density conditions. There are many unknowns when inferring foraging efficiencies, including uncertainties in assimilation efficiency, how ODBA scales with shark size, and, critically, how swim speed scales with shark size. Some of these aspects could not be tested using our data, unfortunately, but technology exists to supplement tagging studies in the future. For example, the use of tags with speed sensors sensitive to low speed, the use of photogrammetric data to estimate shark length (Johnston, 2019), and the use of on-animal cameras to confirm foraging periods as well as to determine under what conditions and in what manner active suction is employed, could all enhance future studies. Additionally,

Journal of Experimental Biology (2020) 223, jeb224402. doi:10.1242/jeb.224402

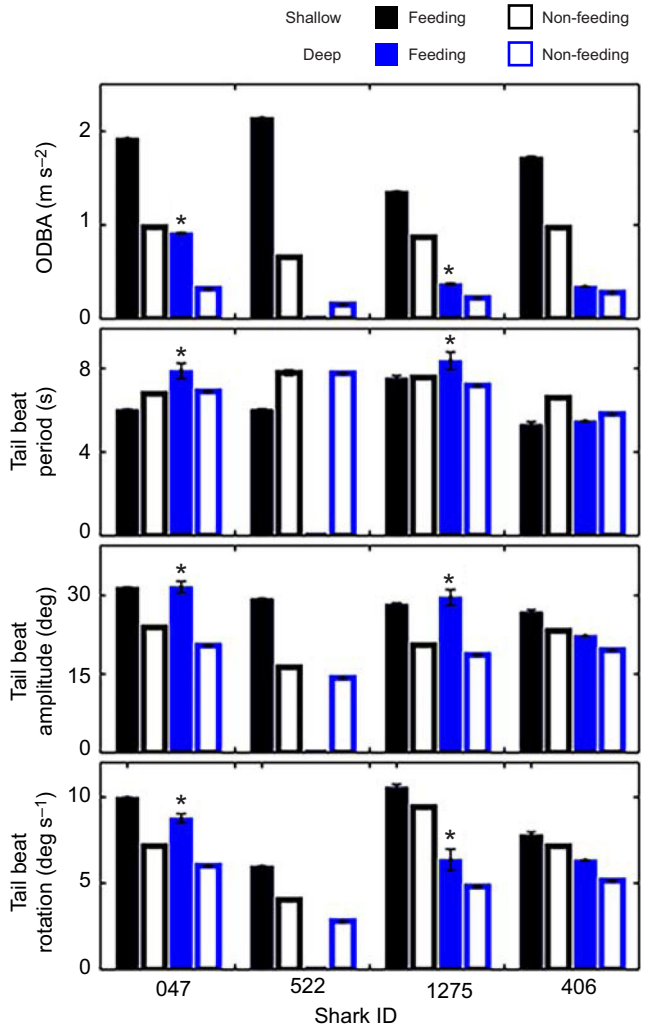

Fig. 6. Surface and sub-surface foraging energetics. *Sharks that spent <1% of their foraging time at depth. Error bars are 95% confidence intervals.

future studies that seek to elucidate the overall foraging efficiency of whale sharks would do well to collocate accelerometer enabled tagging efforts with simultaneous prey density measurements at the depths of observed foraging. We observed diverse foraging tactics among our four tag deployments, but because we did not have simultaneous prey measurements, we could not determine the degree to which these differences reflect individual behavioral choices or instead reflect differences in prey availability.

Although this study utilized OpenTags to elucidate shark behavior, this generation of OpenTag may need improvements in sensor stability before it should be relied on for further studies. From nine recovered tags, we had only four give readable records. Within those four, several analytical problems arose within the tag records. For all deployments, pressure and temperature are stored in a separate file from the accelerometer data. In all files, there is a variably sized gap (usually <2 s) between where one file ends and where the next begins, probably as a result of file write processes within the tag, and this gap also varies between the two concurrently recorded files. We wrote a script, available from https://purl.stanford.edu/dp151fd3984, to read in OpenTag files, synchronize the two types of files, and interpolate between the gaps, but would recommend that any potential users are familiar with the limitations of the device before relying on OpenTags for critical data.

Recent developments in bio-logging device sensors have led to increased availability of these sensors at a variety of cost points depending on need (Fahlbusch and Harrington, 2019). We deployed the open-source OpenTag system on ten sharks from 2013 to 2016 with mixed success. The attachments used elastic bands on the first dorsal fin and the observed reactions to the tagging events were minimal, although this may represent a potential bias as animals prone to reaction were not approached. Gleiss et al. (2009) deployed similar devices on the second dorsal fins of whale sharks in Western Australia using a clamp and latch and noted a dive response in nine of 10 sharks with substantial initial tagging reactions in three animals. The muted responses of our animals could be due to the softer attachment (elastic bands) versus the metal clamps used in the previous study, or could also be due in part to the habituation of the sharks in the Yucatán to human divers. Having a consistent attachment point allows for comparisons of body rotation and ODBA, both metrics that are sensitive to tag placement. The first dorsal fin does have some stability issues that had to be filtered out in post-processing, but this attachment point allows for both calculation of stroke rates as well as body orientation, so we would recommend this deployment location for future studies, although ideally placing the tag as close to the base of the dorsal fin as possible to minimize fin wobble.

The depth data from these long-term deployments also proved enlightening. Whale sharks spend a substantial portion of time descending or ascending or swimming at depth, even directly proximal to feeding periods (Fig. 4). This is important because it means we are likely to be under-estimating the abundance of whale sharks when using typical surface or aerial assessments of populations. IMU data indicate that whale sharks spend 68±20% of their time away from the surface during daylight hours, which warrants application of a multiplicative correction factor of ∼3 for estimating abundance from surface assessments at this site, at least for surveys not undertaken during intensive surface foraging, when most of the population is probably taking advantage of high-quality food.

In addition to swimming forward at a consistent depth, we found that the whale sharks in our study also regularly performed ‘bounce dives’ in which they took advantage of their negative buoyancy to glide with minimal stroking on descent and then ascend while stroking (Fig. 4). We also observed the converse, where the shark first ascended from depth and then followed that maneuver with a gliding descent (Fig. 4). Bounce dives are an enigmatic, but consistently observed feature of shark elasmobranch behavior that is probably related to energy conservation while gliding and thermal regulation in colder water to reduce metabolic rate (Gleiss et al., 2011a; Thums et al., 2013), but could also be related to surveying the water column for the presence of sufficient food. As we found that sub-surface feeding is less costly than surface feeding, locating sub-surface thin layers of zooplankton (Benoit-Bird et al., 2009) may assist energy acquisition at low cost, and may allow for foraging at lower prey densities.

Given the increased energetic costs of filter feeding, it is only efficient to do so if prey conditions are sufficiently high. Whale sharks, like other large filter feeders (Ashjian et al., 2010; Findlay et al., 2017; Crowe et al., 2018), form aggregations spatially and temporally collocated where and when dense concentrations of potential prey can be found (Hoffmayer et al., 2007; de la Parra Venegas et al., 2011; Norman et al., 2017). The Afuera aggregation of whale sharks in our study area appears annually at the northeastern tip of the Yucatán Peninsula from May to September, largely coincident with increased zooplankton at the

Journal of Experimental Biology (2020) 223, jeb224402. doi:10.1242/jeb.224402

Fig. 7. Compass orientation of sharks when feeding and not feeding.

surface (de la Parra Venegas et al., 2011). Although the precise contribution of these foraging periods to the overall energy budgets of these sharks is unknown, it is likely, based on the aggregations they draw, that they form a substantial contribution of the overall energy intake of Yucatán whale sharks. Observed foraging bouts were as long as 11 h, implying that whale sharks probably feed for as long as prey conditions are good. Given that in 397 h of tag data we identified only 78 h of feeding (20% of the total time), and the four sharks averaged 5.0±2.2 h per day foraging, if shark foraging is interrupted by tourist boat activity, which typically spend around 3 h among the aggregation, it could represent a substantial interruption of foraging while conditions are good. Although the sharks we tagged appear to be feeding for ∼20 times longer each day than whale sharks investigated in Australia by Gleiss et al. (2013), it should be noted that (a) reported foraging behavior in the Australian study was limited to identification of vertical feeding (high pitch angle) on discrete surface patches of krill, and (b) foraging period identification in that study was limited to times when dynamic body acceleration was greater than the 90th percentile of the overall deployment record, implying that even if no other criteria were considered, no more than 10% of total time could be identified as foraging using their method. As such, we consider our approach to

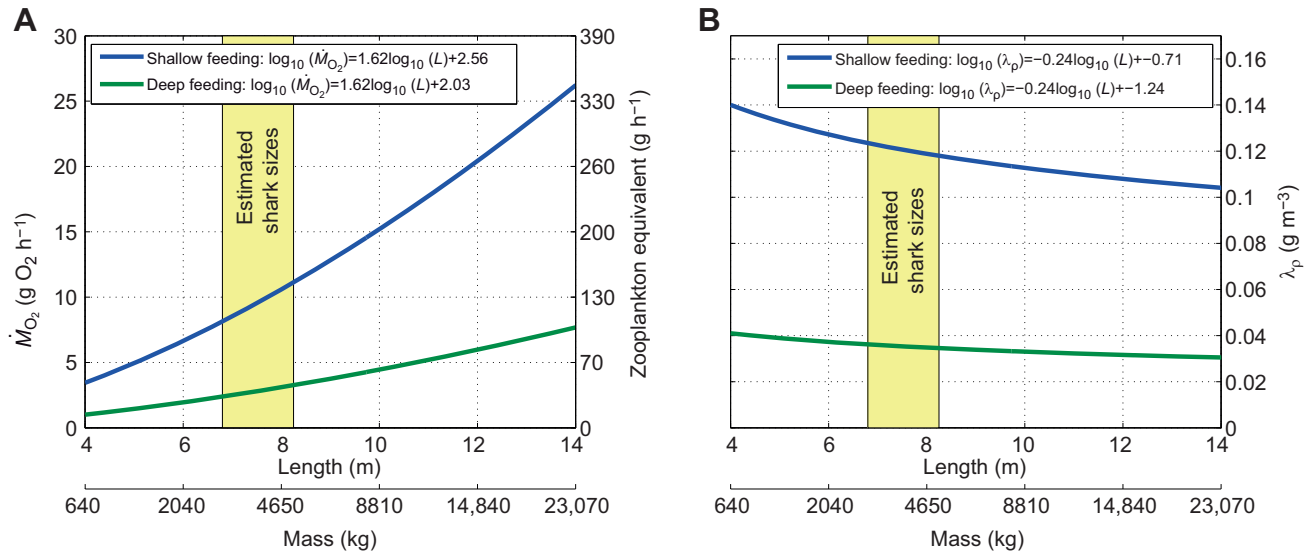

Fig. 8. Increased cost of foraging at depth and at the surface, based on increase in ODBA. The highlighted region represents the approximate range of shark sizes tagged in this study, estimated by researchers at the time of tag attachment. (A) Calculated metabolic rate ($\dot{M}_{O_2}$) and the equivalent amount of zooplankton that should be consumed for a shark of a given size. *Y*-axis units are in g O_2 h^{-1} for clarity, while the listed equation matches the text and maintains mg O_2 h^{-1}. (B) Minimum mean patch density (λ_p) that would have to be consumed for a shark of a given size to recover the increased energy spent for locomotion when ram filter feeding. *L*, shark length.

be a more generally applicable method for identifying periods of ram filtration feeding in whale shark accelerometer data.

It should also be noted that feeding effort of whale sharks in the Afuera aggregation has generally been interpreted from surface observations to be between 08:00 h and about 14:00–15:00 h, with peak activity between 09:00 h and 12:00 h. However, our four sharks did not conform to this pattern. While we did observe a higher proportion of foraging from 09:00 h to 12:00 h (Fig. 9), we also observed surface foraging in the pre-dawn hours and throughout the day, and we observed sub-surface feeding throughout both day and night-time hours. More research with these non-invasive tags may be necessary to determine if the general interpretation of diel foraging effort is influenced by human observers in the area.

In addition to potential impacts from disturbance, whale sharks are also vulnerable to direct human injury through vessel strikes. We found that whale sharks spend a considerable amount of time on the surface during the day (Table 1). In other locations, sometimes more than a quarter of whale sharks have detectable scars indicating past boat strike injuries (Womersley et al., 2016), which is roughly consistent with our observations at the Afuera site since 2009, where 13–30% of individuals show unique scarring patterns (Ramírez-Macías et al., 2012). Risk of boat strike should be incorporated into management practices, including codes of conduct and interactions guidelines, for all whale shark tourism activities.

In warm tropical waters, oxygen is less available than in temperate climates and is expected to decrease as ocean temperatures continue to warm (Matear and Hirst, 2003; Shaffer et al., 2009). Due to lower food availability and lower abilities to extract oxygen, habitat for large ectotherms shrinks in warming oceans (Sheridan and Bickford, 2011; Penn et al., 2018). Indeed, in prior mass extinction events, large ectotherms were some of the most affected by deoxygenation from warming ocean waters (Daufresne et al., 2009; Belben et al., 2017). As it is likely that whale sharks will be similarly affected by the current trends, particularly given the increased energetic costs associated with their foraging style noted in this study, there is an urgent need for more detailed investigation into the energetic balancing act played out by the world's largest fish in tropical ocean waters.

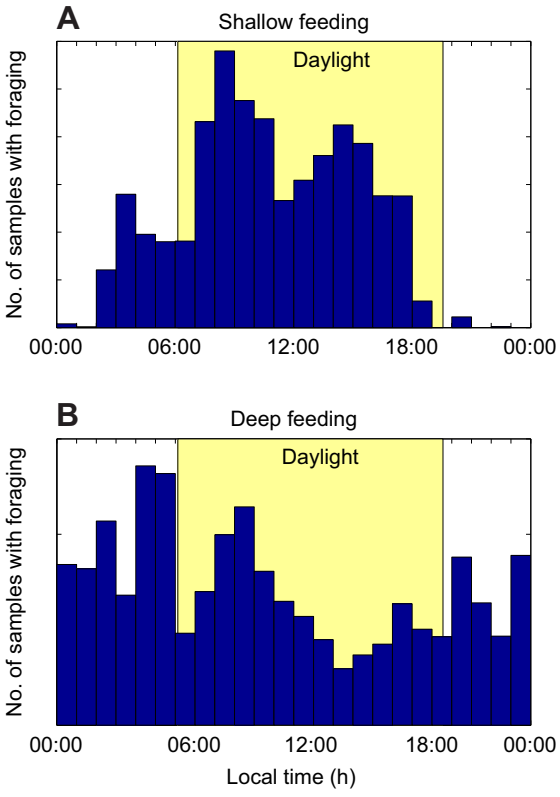

Fig. 9. Histogram of identified foraging periods for shallow and deep feeding. (A) Shallow feeding; (B) deep feeding.

Acknowledgements
We appreciate the support of the staff of Caribbean Connection in Cancún, CONANP/SEMARNAT in the Mexican Federal Government, and Kerry Gladish and the staff and volunteers of the Georgia Aquarium. Beatriz Galvan and Emilio and Eugenio de la Parra provided invaluable field assistance. Colin Ware provided technical support on the 2015 field trip.

Competing interests
The authors declare no competing or financial interests.

Author contributions
Conceptualization: J.J.L., R.C., R.d.l.P., D.H.W., A.D.M.D.; Methodology: D.E.C., R.d.l.P., A.D.M.D.; Software: D.E.C.; Validation: D.E.C., A.D.M.D.; Formal analysis: D.E.C., A.D.M.D.; Investigation: J.J.L., R.C., R.d.l.P, D.H.W., A.D.M.D..; Data curation: J.J.L., R.C., R.d.l.P.;Writing - original draft: D.E.C.; Writing - review & editing: D.E.C., J.J.L., R.C., R.d.l.P., D.H.W., A.D.M.D.; Supervision: D.H.W., A.D.M.D.; Project administration: J.J.L.; Funding acquisition: J.J.L., A.D.M.D.

Funding
This research was supported by Georgia Aquarium Research and Conservation funds.

Data availability
MATLAB data files used for analysis, a script for importing OpenTag data into MATLAB file format (Supplemental Code S1), and example raw data for this process are publicly available at Stanford's digital repository: https://purl.stanford.edu/dp151fd3984

References

Ashjian, C. J., Braund, S. R., Campbell, R. G., George, J. C. C., Kruse, J., Maslowski, W., Moore, S. E., Nicolson, C. R., Okkonen, S. R., Sherr, B. F. et al. (2010). Climate variability, oceanography, bowhead whale distribution, and Iñupiat subsistence whaling near Barrow, Alaska. *Arctic* **63**, 179-194. doi:10.14430/arctic973

Belben, R. A., Underwood, C. J., Johanson, Z. and Twitchett, R. J. (2017). Ecological impact of the end-Cretaceous extinction on lamniform sharks. *PLoS ONE* **12**, e0178294. doi:10.1371/journal.pone.0178294

Benoit-Bird, K. J., Cowles, T. J. and Wingard, C. E. (2009). Edge gradients provide evidence of ecological interactions in planktonic thin layers. *Limnol. Oceanogr.* **54**, 1382-1392. doi:10.4319/lo.2009.54.4.1382

Blake, R. W. (2009). Biological implications of the hydrodynamics of swimming at or near the surface and in shallow water. *Bioinspir. Biomim.* **4**, 015004. doi:10.1088/1748-3182/4/1/015004

Brena, P. F., Mourier, J., Planes, S. and Clua, E. (2015). Shark and ray provisioning: functional insights into behavioral, ecological and physiological responses across multiple scales. *Mar. Ecol. Prog. Ser.* **538**, 273-283. doi:10.3354/meps11492

Cade, D. E., Barr, K. R., Calambokidis, J., Friedlaender, A. S. and Goldbogen, J. A. (2018). Determining forward speed from accelerometer jiggle in aquatic environments. *J. Exp. Biol.* **221**, jeb170449. doi:10.1242/jeb.170449

Cade, D. E., Carey, N., Domenici, P., Potvin, J. and Goldbogen, J. A. (2020). Predator-informed looming stimulus experiments reveal how large filter feeding whales capture highly maneuverable forage fish. *Proc. Natl Acad. Sci. USA* **117**, 472-478. doi:10.1073/pnas.1911099116

Cade, D. E., Friedlaender, A. S., Calambokidis, J. and Goldbogen, J. A. (2016). Kinematic diversity in rorqual whale feeding mechanisms. *Curr. Biol.* **26**, 2617-2624. doi:10.1016/j.cub.2016.07.037

Carey, N. and Goldbogen, J. A. (2017). Kinematics of ram filter feeding and beat-glide swimming in the northern anchovy *Engraulis mordax*. *J. Exp. Biol.* **220**, 2717-2725. doi:10.1242/jeb.158337

Carlson, J. K., Goldman, K. J. and Lowe, C. G. (2004). Metabolism, energetic demand, and endothermy. In *Biology of Sharks and Their Relatives*, vol. 10 (ed. J. C. Carrier, J. A. Musick and M. R. Heithaus), pp. 269-286. Taylor and Francis.

Carrier, J. C., Musick, J. A. and Heithaus, M. R. (2012). *Biology of Sharks and Their Relatives*. CRC press.

Chen, C.-T., Liu, K. M. and Joung, S. J. (2002). Preliminary report on Taiwan's whale shark fishery. In *Elasmobranch Biodiversity, Conservation and Management: Proceedings of the International Seminar and Workshop, Sabah, Malaysia*, July 1997, pp. 162-167. IUCN Gland, Switzerland.

Colman, J. G. (1997). A review of the biology and ecology of the whale shark. *J. Fish Biol.* **51**, 1219-1234. doi:10.1111/j.1095-8649.1997.tb01138.x

Crowe, L. M., O'brien, O., Curtis, T. H., Leiter, S. M., Kenney, R. D., Duley, P. and Kraus, S. D. (2018). Characterization of large basking shark *Cetorhinus maximus* aggregations in the western North Atlantic Ocean. *J. Fish Biol.* **92**, 1371-1384. doi:10.1111/jfb.13592

Daufresne, M., Lengfellner, K. and Sommer, U. (2009). Global warming benefits the small in aquatic ecosystems. *Proc. Natl Acad. Sci. USA* **106**, 12788-12793. doi:10.1073/pnas.0902080106

de la Parra Venegas, R., Hueter, R., Cano, J. G., Tyminski, J., Remolina, J. G., Maslanka, M., Ormos, A., Weigt, L., Carlson, B. and Dove, A. (2011). An unprecedented aggregation of whale sharks, *Rhincodon typus*, in Mexican coastal waters of the Caribbean Sea. *PLoS ONE* **6**, e18994. doi:10.1371/journal.pone.0018994

Duffy, C. A. J. (2002). Distribution, seasonality, lengths, and feeding behaviour of whale sharks (*Rhincodon typus*) observed in New Zealand waters. *N. Z. J. Mar. Freshw. Res.* **36**, 565-570. doi:10.1080/00288330.2002.9517112

Durbin, A., Durbin, E. G., Verity, P. G. and Smayda, T. J. (1980). Voluntary swimming speeds and respiration rates of a filter-feeding planktivore, the Atlantic Menhaden, *Brevoortia tyrannus* (Pisces: Clupeidae). *Fish. Bull.* **78**, 877.

Fahlbusch, J. A. and Harrington, K. J. (2019). A low-cost, open-source inertial movement GPS logger for eco-physiology applications. *J. Exp. Biol.* **222**, jeb211136. doi:10.1242/jeb.211136

Findlay, K. P., Seakamela, S. M., Meÿer, M. A., Kirkman, S. P., Barendse, J., Cade, D. E., Hurwitz, D., Kennedy, A. S., Kotze, P. G. H., McCue, S. A. et al. (2017). Humpback whale 'super-groups' – a novel low-latitude feeding behaviour of Southern Hemisphere humpback whales (*Megaptera novaeangliae*) in the Benguela Upwelling System. *PLoS ONE* **12**, e0172002. doi:10.1371/journal.pone.0172002

Fossette, S., Gleiss, A. C., Chalumeau, J., Bastian, T., Armstrong, C. D., Vandenabeele, S., Karpytchev, M. and Hays, G. C. (2015). Current-oriented swimming by jellyfish and its role in bloom maintenance. *Curr. Biol.* **25**, 342-347. doi:10.1016/j.cub.2014.11.050

Friedman, M., Shimada, K., Martin, L. D., Everhart, M. J., Liston, J., Maltese, A. and Triebold, M. (2010). 100-million-year dynasty of giant planktivorous bony fishes in the Mesozoic seas. *Science* **327**, 990-993. doi:10.1126/science.1184743

Gearty, W., McClain, C. R. and Payne, J. L. (2018). Energetic tradeoffs control the size distribution of aquatic mammals. *Proc. Natl Acad. Sci. USA* **115**, 4194-4199. doi:10.1073/pnas.1712629115

Gill, T. (1905). On the habits of the great whale shark (*Rhineodon typus*). *Science* **21**, 790-791. doi:10.1126/science.21.542.790

Gleiss, A. C., Norman, B., Liebsch, N., Francis, C. and Wilson, R. P. (2009). A new prospect for tagging large free-swimming sharks with motion-sensitive data-loggers. *Fish. Res.* **97**, 11-16. doi:10.1016/j.fishres.2008.12.012

Gleiss, A. C., Norman, B. and Wilson, R. P. (2011a). Moved by that sinking feeling: variable diving geometry underlies movement strategies in whale sharks. *Funct. Ecol.* **25**, 595-607. doi:10.1111/j.1365-2435.2010.01801.x

Gleiss, A. C., Wilson, R. P. and Shepard, E. L. C. (2011b). Making overall dynamic body acceleration work: on the theory of acceleration as a proxy for energy expenditure. *Methods Ecol. Evol.* **2**, 23-33. doi:10.1111/j.2041-210X.2010.00057.x

Gleiss, A. C., Wright, S., Liebsch, N., Wilson, R. P. and Norman, B. (2013). Contrasting diel patterns in vertical movement and locomotor activity of whale sharks at Ningaloo Reef. *Mar. Biol.* **160**, 2981-2992. doi:10.1007/s00227-013-2288-3

Goldbogen, J. A. (2018). Physiological constraints on marine mammal body size. *Proc. Natl Acad. Sci. USA* **115**, 3995-3997. doi:10.1073/pnas.1804077115

Goldbogen, J. A., Cade, D. E., Wisniewska, D. M., Potvin, J., Segre, P. S., Savoca, M. S., Hazen, E. L., Czapanskiy, M. F., Kahane-Rapport, S. R., DeRuiter, S. L. et al. (2019). Why whales are big but not bigger: physiological drivers and ecological limits in the age of ocean giants. *Science* **366**, 1367-1372. doi:10.1126/science.aax9044

Gough, W. T., Segre, P. S., Bierlich, K., Cade, D. E., Potvin, J., Fish, F. E., Dale, J., di Clemente, J., Friedlaender, A. S., Johnston, D. W. et al. (2019). Scaling of swimming performance in baleen whales. *J. Exp. Biol.* **222**, jeb204172. doi:10.1242/jeb.204172

Gudger, E. W. (1941a). The feeding organs of the whale shark, *Rhineodon typus*. *J. Morphol.* **68**, 81-99. doi:10.1002/jmor.1050680105

Gudger, E. W. (1941b). The food and feeding habits of the whale shark, *Rhineodon typus*. *J. Elisha Mitchell Sci. Soc.* **57**, 57-72.

Haines, G. E. and Sanderson, S. L. (2017). Integration of swimming kinematics and ram suspension feeding in a model American paddlefish, *Polyodon spathula*. *J. Exp. Biol.* **220**, 4535-4547. doi:10.1242/jeb.166835

Hoffmayer, E. R., Franks, J. S., Driggers, W. B., III, Oswald, K. J. and Quattro, J. M. (2007). Observations of a feeding aggregation of whale sharks, *Rhincodon typus*, in the north central Gulf of Mexico. *Gulf Caribb. Res.* **19**, 69-73. doi:10.18785/gcr.1902.08

Hsu, H. H., Joung, S. J. and Liu, K. M. (2012). Fisheries, management and conservation of the whale shark *Rhincodon typus* in Taiwan. *J. Fish Biol.* **80**, 1595-1607. doi:10.1111/j.1095-8649.2012.03234.x

Johnson, M. P. and Tyack, P. L. (2003). A digital acoustic recording tag for measuring the response of wild marine mammals to sound. *IEEE J. Ocean. Eng.* **28**, 3-12. doi:10.1109/JOE.2002.808212

Johnston, D. W. (2019). Unoccupied aircraft systems in marine science and conservation. *Annu. Rev. Mar. Sci.* **11**, 439-463. doi:10.1146/annurev-marine-010318-095323

Kao, J. S. (2000). *Diet, Daily Ration and Gastric Evacuation of the Leopard shark (Triakis semifasciata)*. Hayward: Calif. State University.

Ketchum, J. T., Galván-Magaña, F. and Klimley, A. P. (2013). Segregation and foraging ecology of whale sharks, *Rhincodon typus*, in the southwestern Gulf of California. *Environ. Biol. Fishes* **96**, 779-795. doi:10.1007/s10641-012-0071-9

Kjerfve, B. (1994). *Coastal oceanographic characteristics: Cancun-Tulum corridor, Quintana Roo*. Final Report, Programa de Ecologia, Pesquerias y Oceanografia del Golfo de Mexico, Universidad Autonoma de Campeche, pp. 1-35. Universidad Autónoma de Campeche.

Lawson, C. L., Halsey, L. G., Hays, G. C., Dudgeon, C. L., Payne, N. L., Bennett, M. B., White, C. R. and Richardson, A. J. (2019). Powering ocean giants: the energetics of shark and ray megafauna. *Trends Ecol. Evol.* **34**, 1009-1021. doi:10.1016/j.tree.2019.07.001

Lear, K. O., Whitney, N. M., Brewster, L. R., Morris, J. J., Hueter, R. E. and Gleiss, A. C. (2017). Correlations of metabolic rate and body acceleration in three species of coastal sharks under contrasting temperature regimes. *J. Exp. Biol.* **220**, 397-407. doi:10.1242/jeb.146993

Leigh, S. C., Papastamatiou, Y. and German, D. P. (2017). The nutritional physiology of sharks. *Rev. Fish Biol. Fish.* **27**, 561-585. doi:10.1007/s11160-017-9481-2

Matear, R. J. and Hirst, A. C. (2003). Long-term changes in dissolved oxygen concentrations in the ocean caused by protracted global warming. *Global Biogeochem. Cycles* **17**. doi:10.1029/2002GB001997

McArdle, W. D., Katch, F. I. and Katch, V. L. (2010). *Exercise Physiology: Nutrition, Energy, and Human Performance*: Lippincott Williams & Wilkins.

Meekan, M. G., Fuiman, L. A., Davis, R., Berger, Y. and Thums, M. (2015). Swimming strategy and body plan of the world's largest fish: implications for foraging efficiency and thermoregulation. *Front. Mar. Sci.* **2**, 64. doi:10.3389/fmars.2015.00064

Merino, M. (1998). Upwelling on the Yucatan Shelf: hydrographic evidence. *J. Mar. Syst.* **13**, 101-122. doi:10.1016/S0924-7963(96)00123-6

Motta, P. J., Maslanka, M., Hueter, R. E., Davis, R. L., De la Parra, R., Mulvany, S. L., Habegger, M. L., Strother, J. A., Mara, K. R., Gardiner, J. M. et al. (2010). Feeding anatomy, filter-feeding rate, and diet of whale sharks *Rhincodon typus* during surface ram filter feeding off the Yucatan Peninsula, Mexico. *Zoology* **113**, 199-212. doi:10.1016/j.zool.2009.12.001

Nelson, J. D. and Eckert, S. A. (2007). Foraging ecology of whale sharks (*Rhincodon typus*) within Bahía de los Angeles, Baja California Norte, México. *Fish. Res.* **84**, 47-64. doi:10.1016/j.fishres.2006.11.013

Noda, T., Kikuchi, D. M., Takahashi, A., Mitamura, H. and Arai, N. (2016). Pitching stability of diving seabirds during underwater locomotion: a comparison among alcids and a penguin. *Animal Biotelemetry* **4**, 10. doi:10.1186/s40317-016-0102-y

Norman, B. and Catlin, J. (2007). *Economic importance of conserving whale sharks*. Report for the international fund for animal welfare (IFAW), Australia.

Norman, B. M., Holmberg, J. A., Arzoumanian, Z., Reynolds, S. D., Wilson, R. P., Rob, D., Pierce, S. J., Gleiss, A. C., de la Parra, R., Galvan, B. et al. (2017). Undersea constellations: the global biology of an endangered marine megavertebrate further informed through citizen science. *Bioscience* **67**, 1029-1043. doi:10.1093/biosci/bix127

Penn, J. L., Deutsch, C., Payne, J. L. and Sperling, E. A. (2018). Temperature-dependent hypoxia explains biogeography and severity of end-Permian marine mass extinction. *Science* **362**, eaat1327. doi:10.1126/science.aat1327

Potvin, J. and Werth, A. J. (2017). Oral cavity hydrodynamics and drag production in Balaenid whale suspension feeding. *PLoS ONE* **12**, e0175220. doi:10.1371/journal.pone.0175220

Ramírez-Macías, D., Meekan, M., de La Parra-Venegas, R., Remolina-Suárez, F., Trigo-Mendoza, M. and Vázquez-Juárez, R. (2012). Patterns in composition, abundance and scarring of whale sharks *Rhincodon typus* near Holbox Island, Mexico. *J. Fish Biol.* **80**, 1401-1416. doi:10.1111/j.1095-8649.2012.03258.x

Rowat, D. and Brooks, K. S. (2012). A review of the biology, fisheries and conservation of the whale shark *Rhincodon typus*. *J. Fish Biol.* **80**, 1019-1056. doi:10.1111/j.1095-8649.2012.03252.x

Sanderson, S. L. and Wassersug, R. (1990). Suspension-feeding vertebrates. *Sci. Am.* **262**, 96-102. doi:10.1038/scientificamerican0390-96

Sanderson, S. L., Cech, S. and Cheer, A. (1994). Paddlefish buccal flow velocity during ram suspension feeding and ram ventilation. *J. Exp. Biol.* **186**, 145-156.

Schleimer, A., Araujo, G., Penketh, L., Heath, A., McCoy, E., Labaja, J., Lucey, A. and Ponzo, A. (2015). Learning from a provisioning site: code of conduct

compliance and behaviour of whale sharks in Oslob, Cebu, Philippines. *PeerJ* **3**, e1452. doi:10.7717/peerj.1452

Schmidt-Nielsen, K. and Knut, S.-N. (1984). *Scaling: Why is Animal Size so Important?*: Cambridge University Press.

Shaffer, G., Olsen, S. M. and Pedersen, J. O. P. (2009). Long-term ocean oxygen depletion in response to carbon dioxide emissions from fossil fuels. *Nat. Geosci.* **2**, 105. doi:10.1038/ngeo420

Sheridan, J. A. and Bickford, D. (2011). Shrinking body size as an ecological response to climate change. *Nat. Climate Change* **1**, 401. doi:10.1038/nclimate1259

Simon, M., Johnson, M., Tyack, P. and Madsen, P. T. (2009). Behaviour and kinematics of continuous ram filtration in bowhead whales (*Balaena mysticetus*). *Proc. R. Soc. B* **276**, 3819-3828. doi:10.1098/rspb.2009.1135

Sims, D. W. (2000). Filter-feeding and cruising swimming speeds of basking sharks compared with optimal models: they filter-feed slower than predicted for their size. *J. Exp. Mar. Biol. Ecol.* **249**, 65-76. doi:10.1016/S0022-0981(00)00183-0

Slater, G. J., Goldbogen, J. A. and Pyenson, N. D. (2017). Independent evolution of baleen whale gigantism linked to Plio-Pleistocene ocean dynamics. *Proc. R. Soc. B* **284**, 20170546. doi:10.1098/rspb.2017.0546

Stevens, J. D. (2007). Whale shark (*Rhincodon typus*) biology and ecology: a review of the primary literature. *Fish. Res.* **84**, 4-9. doi:10.1016/j.fishres.2006.11.008

Taylor, L. R., Compagno, L. J. V. and Struhsaker, P. J. (1983). Megamouth-a new species, genus and a new family of lamnoid sharks (*Megachasmia pelagios*, family Megachasmidae) from the Hawaiian Islands. *Proc. California Acad. Sci.* **43**, 87-110.

Thums, M., Meekan, M., Stevens, J., Wilson, S. and Polovina, J. (2013). Evidence for behavioural thermoregulation by the world's largest fish. *J. R. Soc. Interface* **10**, 20120477. doi:10.1098/rsif.2012.0477

Tomita, T., Sato, K., Suda, K., Kawauchi, J. and Nakaya, K. (2011). Feeding of the megamouth shark (Pisces: Lamniformes: Megachasmidae) predicted by its hyoid arch: a biomechanical approach. *J. Morphol.* **272**, 513-524. doi:10.1002/jmor.10905

van der Hoop, J. M., Nousek-McGregor, A. E., Nowacek, D. P., Parks, S. E., Tyack, P. and Madsen, P. T. (2019). Foraging rates of ram-filtering North Atlantic right whales. *Funct. Ecol.* **33**, 1290-1306. doi:10.1111/1365-2435.13357

Vogel, S. (1994). *Life in Moving Fluids: the Physical Biology of Flow*: Princeton University Press.

Ware, C., Arsenault, R., Plumlee, M. and Wiley, D. (2006). Visualizing the underwater behavior of humpback whales. *IEEE Comput. Graph. Appl.* **26**, 14-18. doi:10.1109/MCG.2006.93

Ware, C., Trites, A. W., Rosen, D. A. S. and Potvin, J. (2016). Averaged propulsive body acceleration (APBA) can be calculated from biologging tags that incorporate gyroscopes and accelerometers to estimate swimming speed, hydrodynamic drag and energy expenditure for Steller sea lions. *PLoS ONE* **11**, e0157326. doi:10.1371/journal.pone.0157326

Whitney, N. M., Papastamatiou, Y. P., Holland, K. N. and Lowe, C. G. (2007). Use of an acceleration data logger to measure diel activity patterns in captive whitetip reef sharks, *Triaenodon obesus*. *Aquat. Living Resour.* **20**, 299-305. doi:10.1051/alr:2008006

Williams, T. M. (2019). The biology of big. *Science* **366**, 1316-1317. doi:10.1126/science.aba1128

Wilson, R. P., Liebsch, N., Davies, I. M., Quintana, F., Weimerskirch, H., Storch, S., Lucke, K., Siebert, U., Zankl, S., Müller, G. et al. (2007). All at sea with animal tracks; methodological and analytical solutions for the resolution of movement. *Deep Sea Res. Part II Top. Stud. Oceanogr.* **54**, 193-210. doi:10.1016/j.dsr2.2006.11.017

Wilson, R. P., Börger, L., Holton, M. D., Scantlebury, D. M., Gómez-Laich, A., Quintana, F., Rosell, F., Graf, P. M., Williams, H., Gunner, R. et al. (2020). Estimates for energy expenditure in free-living animals using acceleration proxies: a reappraisal. *J. Anim. Ecol.* **89**, 161-172. doi:10.1111/1365-2656.13040

Womersley, F. C., Leblond, S. T. and Rowat, D. R. (2016). Scarring instance and healing capabilities of whale sharks and possible implications. In The 4th International Whale Shark Conference, vol. 2016, p. 67. Hamad bin Khalifa University Press (HBKU Press).

Wright, S., Metcalfe, J. D., Hetherington, S. and Wilson, R. (2014). Estimating activity-specific energy expenditure in a teleost fish, using accelerometer loggers. *Mar. Ecol. Prog. Ser.* **496**, 19-32. doi:10.3354/meps10528

Yowell, D. W. and Vinyard, G. L. (1993). An energy-based analysis of particulate-feeding and filter-feeding by blue tilapia, *Tilapia aurea*. *Environ. Biol. Fishes* **36**, 65-72. doi:10.1007/BF00005980